Computer Visualization of Vortex Wake Systems

Roger C. Strawn*
U.S. Army Aviation and Missile Command, Moffett Field, California 94035-1000
David N. Kenwright†
MRJ Technology Solutions, Moffett Field, California 94035-1000
and
Jasim Ahmad‡
MCAT Institute, Moffett Field, California 94035-1000

Introduction

THE general problem of identifying and visualizing free-shear vortex centers in large transient three-dimensional computational fluid dynamics (CFD) data sets is addressed. This vortex identification is particularly important for rotorcraft problems, where the interactions between rotor blades and their vortical wake systems play an important role in determining rotor airloads, noise, and vibrations. These rotorcraft vortices typically consist of an inner core of rotational flow coupled to an irrotational outer flow as modeled by Eq. (1) from Ref. 1:

$$V_\theta = \frac{r\Gamma}{2\pi(r^2 + a^2)} \tag{1}$$

The radius from the vortex center is given by r, with a rotational core radius given by a. V_θ is the vortex tangential velocity, and Γ is the circulation on the blade, which ultimately determines the vortex strength. Beyond the core radius, the velocity field rapidly becomes irrotational. The vortex center coincides with a local maximum in vorticity magnitude.

References 2–4 describe a variety of methods for vortex identification in three dimensions based on different vortex definitions. In particular, Jeong and Hussain[4] develop a general scheme for identifying vortex core regions for both wall-bounded and free-shear flows. This scheme works well for most applications; however, for the rotorcraft problem, we wish to identify the vortex centers, or skeletons, in addition to the outer surfaces of the vortex cores. The vortex centers are important because these regions have the highest velocity gradients relative to the local flow and, hence, have the greatest influence on the rotor aerodynamics. Also, the traces of vortex centers show where the vortices originate on the rotor blades.

Vortices as Centers of Swirling Flow

There is really no formal definition for a vortex in three dimensions. However, a number of practical techniques have been used to help investigators identify vortices, including the characterization of a vortex as the center of a swirling flow. This model has been used by Sujudi and Haimes[5] as a visualization tool for vortex centers. They tested the eigenvalues and eigenvectors of the velocity rate of deformation tensor $[\partial u_i/(\partial x_j)]$ to determine the direction and the center of any swirling flow. If a swirl center lies inside the cell under examination, then this cell contains a vortex center.

This identification method works well for many practical cases; however, confusion arises when multiple vortices have overlapping rotational cores. Figure 1 shows cross-sectional velocity vector and vorticity plots for a model problem with two identical line vortices inside a unit cube grid. These vortices have the same counterclockwise sense of rotation and overlapping rotational cores. Each vortex has a velocity field defined by Eq. (1) with a rotational core radius of 0.35. The overall velocity field is obtained by superposition of the individual vortex velocities, and although this is an idealized case, it demonstrates what happens in typical CFD data set problems when rotational vortex cores overlap. The velocity vector field in Fig. 1b shows only a single rotational center. A vortex identification technique that searches for centers of swirl will identify only one vortex for this case, and its location will be at the center of the square. Similarly, a vortex identification technique that identifies vortex core surfaces[4] will not delineate two vortex centers. Instead, it will show only a combined vortex core surface.

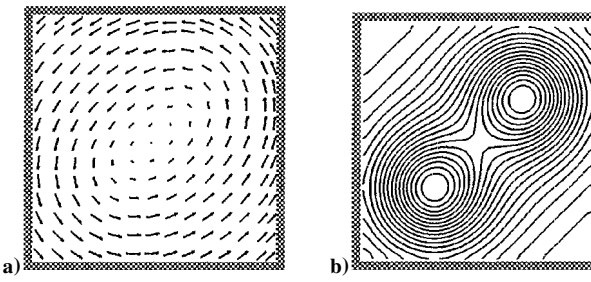

Fig. 1 Velocity vectors and vorticity contours for two line vortices with overlapping rotational cores.

The basic problem is that the combination of rotational vortex velocities does not preserve the center of rotation for each individual vortex. This observation has important implications for rotary-wing calculations, which typically do not have sufficient grid resolution to completely resolve the rotor wake system. This lack of grid resolution causes the computed vortices to artificially diffuse and leads to very large rotational vortex cores, which can easily overlap.

Vortices as Local Maxima of Vorticity Magnitude

Our scheme defines a vortex center as a local maximum of vorticity in a plane that is normal to the vorticity vector. This rules out shear layers, which have high vorticity values but no local vorticity maxima. This idea is similar to that of Banks and Singer,[3] who identified vortex centers as local pressure minima in a plane that is normal to the vorticity vector. For practical simplicity, our implementation searches for local vorticity maxima on the faces of each interior element in a structured hexahedral grid rather than on the exact planes that are normal to the vorticity vector.

We derive nodal values for the fluid vorticity vector $\boldsymbol{\omega}$ from the velocity field $\boldsymbol{u}$, using central differences to compute the velocity derivatives. The subsequent search for local vorticity maxima takes place in uniform computational space to simplify the analysis. The vortex detection scheme extracts blocks of 3×3 hexahedral cells, as shown in Fig. 2. We analyze each face of this central cell and its surrounding nodes in turn. The first step is a candidate test to determine whether a local maximum exists on or near the central face. If the vorticity magnitude is highest at one of the central vertices of the 4×4 nodal patch, then the central face is a candidate for a vorticity maximum.

The second step determines the exact location of the maximum via the solution of two nonlinear simultaneous equations. The center is located where the gradients of the vorticity magnitude are zero. Construction of these nonlinear equations requires that we also compute values for the gradients of vorticity at each vertex of the central face. We use central differences to compute these gradients, thereby drawing on data only from the 4×4 patch of nodal values. Bilinear functions describe the variation of these gradients over the central face, as shown in Eq. (2). The coefficient values in Eq. (2) can be determined by matching the gradient equations to the known values at the four corners of the face:

$$\begin{aligned} |\omega|_\xi &= a_1 + b_1\xi + c_1\eta + d_1\xi\eta \\ |\omega|_\eta &= a_2 + b_2\xi + c_2\eta + d_2\xi\eta \end{aligned} \tag{2}$$

Received May 26, 1998; revision received Nov. 9, 1998; accepted for publication Dec. 3, 1998. This paper is declared a work of the U.S. Government and is not subject to copyright protection in the United States.

*Research Scientist, Army/NASA Rotorcraft Division, Aeroflightdynamics Directorate. Senior Member AIAA.
†Senior Research Scientist.
‡Research Scientist.

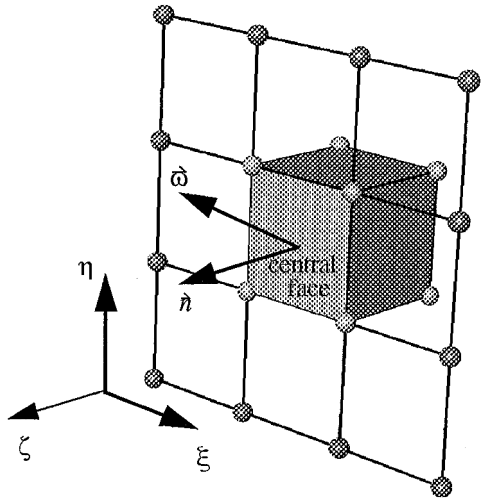

Fig. 2 Tests for local vorticity maxima take place on each face of the central cell in a 3 × 3 × 3 block.

The maximum in vorticity magnitude occurs where $|\omega|_\xi = |\omega|_\eta = 0$. Setting Eqs. (2) to zero and solving them simultaneously gives rise to two quadratic equations for ξ and η. Only one of the roots of each quadratic equation will, in general, lie within the face of the center cell, and we discard the other root. If the computed coordinate (ξ, η) lies inside the central face, then we have found a point in the vortex core. The corresponding coordinates in three-dimensional physical space are obtained from a Jacobian transformation. The procedure finishes when all six faces have been checked for every cell in the mesh. The end result consists of a collection of points that identify the local maxima of vorticity magnitude on cell faces.

In addition to the procedure just described, we use two thresholds to cut down on the number of vortex centers that marginally fit the criteria already described. The first threshold requires that each cell face must have a vorticity magnitude that is larger than a user-determined value. This procedure removes weak vortex centers from the solution. The second threshold addresses the potential for misalignment between a cell-face normal and the vorticity vector on that face. Ideally, the vorticity vector should be aligned with the cell-face normal. Any misalignment can cause a small projection error in the computed vortex center. To avoid these errors, we do not consider a cell face for a vortex center if the angle between the face normal $\boldsymbol{n}$ and the vorticity vector $\boldsymbol{\omega}$ is larger than a user-prescribed threshold of approximately 60 deg. Any vortex center that fails this angle threshold test on a particular cell face will be picked up by other cell faces with better alignment.

We have tested the new vortex detection scheme for the case shown in Fig. 1. Computed vortex traces show two vortex centers that coincide with the two local maximums in vorticity magnitude.

Results and Discussion

We demonstrate our new vortex visualization scheme using two computed solutions. The first case models the steady vortex rollup from a delta wing (Fig. 3). This symmetric case was computed by Chaderjian[6] on a $67 \times 49 \times 107$ grid with a freestream Mach number of 0.27 and an angle of attack of 15 deg. The vorticity-maxima scheme clearly distinguishes what Chaderjian describes as the primary, secondary, and tertiary vortices on each side of the delta wing.

The second test case simulates a wind-tunnel test of the V-22 tiltrotor blades. The solution contains 11 separate overset grids with a total of 1.02×10^6 grid points. The vortex tracing algorithm is applied only in the off-body rotor-wake grids, not in the viscous boundary-layer grids near the rotor blade surfaces. The V-22 blades have a hover-tip Mach number of 0.64, an advance ratio of 0.1, and a shaft tilt of 5 deg. Periodic solutions for this case required approximately 55 CPU hours on a Cray C-90 computer for three revolutions. Figure 4 shows tip and root vortices from each rotor blade that convect below and to the rear of the rotor disk. Figure 4 also shows the overall vortex rollup around the sides of the rotor disk. The vortex identification computations require approximately 6.7×10^{-4} s per hexahedral cell on a Silicon Graphics Onyx II workstation with one 195-MHz R10000 CPU.

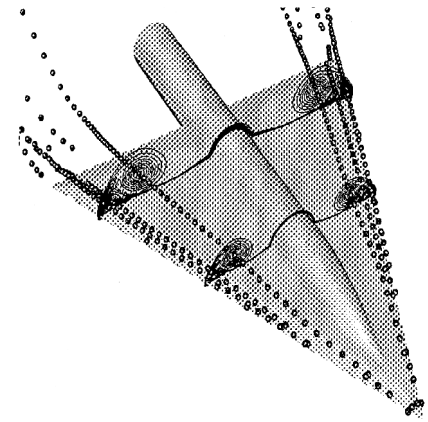

Fig. 3 Vorticity contours and vortex traces on a delta wing.

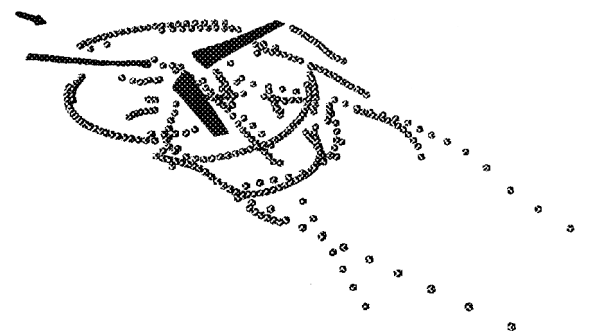

Fig. 4 Vortex core traces for the V-22 rotor blades.

Conclusion

This new vortex detection scheme can identify vortex centers in overlapping regions of rotational flow, and it is easy to implement for structured-grid data sets. In addition to vortex identification, this scheme can be used to guide adaptive-grid CFD methods that seek to locally improve the grid resolution for vortex wake systems. For rotorcraft applications, we expect that visualization tools such as this will become more and more important as solutions on larger computational grids begin to capture more of the fine details of the rotor blade–vortex interactions.

References

[1] Scully, M. P., "Computation of Helicopter Rotor Wake Geometry and Its Influence on Rotor Harmonic Airloads," Massachusetts Inst. of Technology, ASRL TR 178-1, Cambridge, MA, March 1975.

[2] Roth, M., and Peikert, R., "Flow Visualization for Turbomachinery Design," *Proceedings of Visualization '96* (San Francisco, CA), IEEE Computer Society Press, Los Alamitos, CA, 1996, pp. 381–384.

[3] Banks, D. C., and Singer, B. A, "Vortex Tubes in Turbulent Flows: Identification, Representation, Reconstruction," *Proceedings of Visualization '94* (Washington, DC), IEEE Computer Society Press, Los Alamitos, CA, 1994, pp. 132–139.

[4] Jeong, J., and Hussain, F., "On the Identification of a Vortex," *Journal of Fluid Mechanics*, Vol. 285, 1995, p. 69.

[5] Sujudi, D., and Haimes, R., "Identification of Swirling Flow in 3-D Vector Fields," AIAA Paper 95-1715, June 1995.

[6] Chaderjian, N. M., "Navier–Stokes Prediction of Large-Amplitude Delta-Wing Roll Oscillations," *Journal of Aircraft*, Vol. 31, No. 6, 1994, pp. 1333–1340.

A. Plotkin
Associate Editor